

Proton-nucleus elastic scattering and the equation of state of nuclear matter

Kei Iida ^a, Kazuhiro Oyamatsu ^{a,b}, Badawy Abu-Ibrahim ^{a,c}

^a*The Institute of Physical and Chemical Research (RIKEN), Hirosawa, Wako, Saitama 351-0198, Japan*

^b*Department of Media Theories and Production, Aichi Shukutoku University, Nagakute, Nagakute-cho, Aichi-gun, Aichi 480-1197, Japan*

^c*Department of Physics, Cairo University, Giza 12613, Egypt*

Abstract

We calculate differential cross sections for proton-nucleus elastic scattering by using a Glauber theory in the optical limit approximation and nucleon distributions that can be obtained in the framework of macroscopic nuclear models in a way dependent on the equation of state of uniform nuclear matter near the saturation density. We find that the peak angle calculated for unstable neutron-rich nuclei in the small momentum transfer regime increases as the parameter L characterizing the density dependence of the symmetry energy decreases. This is a feature associated with the L dependence of the predicted matter radii.

Key words: Dense matter, Saturation, Unstable nuclei, Elastic scattering

PACS: 21.65.+f, 21.10.Gv, 25.40.Cm

Email address: keiida@riken.go.jp (Kei Iida).

The equation of state (EOS) of nuclear matter is essential to understanding of the saturation property of atomic nuclei [1], the structure of neutron stars [2], the mechanism of stellar collapse [3], and the dynamics of relativistic heavy-ion collisions [4]. Generally, the energy per nucleon of nuclear matter can be expanded around the saturation point of symmetric nuclear matter as

$$w = w_0 + \frac{K_0}{18n_0^2}(n - n_0)^2 + \left[S_0 + \frac{L}{3n_0}(n - n_0) \right] \alpha^2. \quad (1)$$

Here w_0 , n_0 and K_0 are the saturation energy, the saturation density and the incompressibility of symmetric nuclear matter, n is the nucleon density, and $\alpha = 1 - 2x$ is the neutron excess. The parameters L and S_0 characterize the density dependent symmetry energy coefficient $S(n)$: S_0 is the symmetry energy coefficient at $n = n_0$, and $L = 3n_0(dS/dn)_{n=n_0}$ is the symmetry energy density derivative coefficient (hereafter referred to as the “density symmetry coefficient”). As shown in Ref. [1] by describing macroscopic nuclear properties in a manner that is dependent on these EOS parameters, empirical data for masses and radii of stable nuclei can provide a strong constraint on the parameters w_0 , n_0 and S_0 , while leaving K_0 and L uncertain. We remark that the isoscalar giant monopole resonance in nuclei (e.g., Ref. [5]) and caloric curves in nuclear collisions (e.g., Ref. [6]) can constrain K_0 only in a way that is dependent on models for the effective nucleon-nucleon interaction.

The incompressibility K_0 and the density symmetry coefficient L control in which direction the saturation point moves on the density versus energy plane, as the neutron excess increases from zero. This feature can be found from the fact that up to second order in α , the saturation energy w_s and density n_s are given by

$$w_s = w_0 + S_0\alpha^2 \quad (2)$$

and

$$n_s = n_0 - \frac{3n_0L}{K_0}\alpha^2. \quad (3)$$

The influence of K_0 and L on neutron star structure can be significant [7] despite the fact that these parameters characterize the EOS near normal nuclear density and proton fraction, which are fairly small and large, respectively, as compared with the typical densities and proton fractions in the central region of the star.

In our previous investigation [1] we pointed out the possibility that future systematic measurements of the matter radii of unstable neutron-rich nuclei

help derive the value of L . As an example, the matter radii of unstable neutron-rich nuclei such as Ni and even heavier element isotopes are expected to be deduced from future measurements of proton-nucleus elastic differential cross sections that will be performed by using a beam of such nuclei incident on a proton target and detecting scattered protons. This possibility is supported by our finding based on macroscopic nuclear models, which reasonably reproduce empirical data for masses and radii of stable nuclei and allow for uncertainties in the values of K_0 and L , that the matter radii calculated for unstable nuclei depend appreciably on L , while being almost independent of K_0 . However, extraction of the matter radii from experimental data for proton-nucleus elastic differential cross sections and for interaction cross sections is not straightforward in the sense that it requires the approximate scattering theory [8,9]. It is thus instructive to examine how the cross sections themselves are related to the parameter L in a proper theoretical framework.

In this paper we focus on proton-nucleus elastic scattering and, in the optical limit approximation of the Glauber multiple scattering model [10], obtain its angular distribution from the nucleon distributions in a nucleus calculated in Ref. [1] in a way dependent on L and K_0 . For sufficiently high proton incident energies and small momentum transfers to validate the Glauber model, we find that the angle of the scattering peak decreases with L more remarkably for larger neutron excess, while the peak height increases with K_0 almost independently of neutron excess. We suggest the possibility that comparison of the calculations with experimental data for the peak angle may be useful for determination of L .

We begin with macroscopic nuclear models used in this and a previous work [1]. We describe a spherical nucleus of proton number Z and mass number A within the framework of a simplified version of the extended Thomas-Fermi theory [11]. We first write the total energy of a nucleus as a function of the neutron and proton density distributions $n_n(\mathbf{r})$ and $n_p(\mathbf{r})$ in the form

$$E = E_b + E_g + E_C + (A - Z)m_n c^2 + Zm_p c^2, \quad (4)$$

where

$$E_b = \int d^3r n(\mathbf{r}) w(n_n(\mathbf{r}), n_p(\mathbf{r})) \quad (5)$$

is the bulk energy with the energy per nucleon $w(n_n, n_p)$ of uniform nuclear matter,

$$E_g = F_0 \int d^3r |\nabla n(\mathbf{r})|^2 \quad (6)$$

is the gradient energy with adjustable constant F_0 ,

$$E_C = \frac{e^2}{2} \int d^3r \int d^3r' \frac{n_p(\mathbf{r})n_p(\mathbf{r}')}{|\mathbf{r} - \mathbf{r}'|} \quad (7)$$

is the Coulomb energy, and m_n and m_p are the neutron and proton rest masses. We express w as [11]

$$w = \frac{3\hbar^2(3\pi^2)^{2/3}}{10m_n n} (n_n^{5/3} + n_p^{5/3}) + (1 - \alpha^2)v_s(n)/n + \alpha^2 v_n(n)/n, \quad (8)$$

where

$$v_s = a_1 n^2 + \frac{a_2 n^3}{1 + a_3 n} \quad (9)$$

and

$$v_n = b_1 n^2 + \frac{b_2 n^3}{1 + b_3 n} \quad (10)$$

are the potential energy densities for symmetric nuclear matter and pure neutron matter. This expression for w is one of the simplest parametrization that reduces to Eq. (1) in the simultaneous limit of $n \rightarrow n_0$ and $\alpha \rightarrow 0$. We then set the nucleon distributions $n_i(r)$ ($i = n, p$) as

$$n_i(r) = \begin{cases} n_i^{\text{in}} \left[1 - \left(\frac{r}{R_i} \right)^{t_i} \right]^3, & r < R_i, \\ 0, & r \geq R_i, \end{cases} \quad (11)$$

and in the spirit of the Thomas-Fermi approximation minimize the total energy E with respect to R_i , t_i and n_i^{in} with the mass number A , the EOS parameters (n_0, w_0, S_0, K_0, L) and the gradient coefficient F_0 fixed. By calculating the charge number, mass excess and root-mean-square charge radius from the minimizing values of R_i , t_i and n_i^{in} and fitting the results to the empirical values for stable nuclei ($25 \leq A \leq 245$) on the smoothed beta stability line, we finally obtain n_0 , w_0 , S_0 and F_0 for various sets of L and K_0 . We remark that as a result of this fitting, the parameters a_1 - b_2 become functions of K_0 and L , while we fix the remaining parameter b_3 , which controls the EOS of matter for large neutron excess and high density, at 1.58632 fm^3 throughout this fitting process.

The macroscopic nuclear models used here can describe gross nuclear properties such as masses and root-mean-square radii in a manner that is dependent on the EOS parameters, L and K_0 . Notably, as in Ref. [1], these models predict that the root-mean-square matter radii depend appreciably on L , while being almost independent of K_0 . However, there are some limitations in the present macroscopic approach. First, this approach works well in the range of $\alpha \lesssim 0.3$ and $A \gtrsim 50$, where a macroscopic view of the system is relevant. Second, the nuclear surface is not satisfactory in the present Thomas-Fermi-type theory, which tends to underestimate the surface diffuseness and does not allow for the tails of the nucleon distributions. As we shall see, such an underestimated diffuseness has consequence to calculations of proton-nucleus differential cross sections. Lastly, no shell and pairing effects are included.

We proceed to calculate differential cross sections for proton elastic scattering off nuclei using the Glauber theory in the optical limit approximation. The elastic differential cross section at given momentum transfer \mathbf{q} and incident proton energy T_p can be written as (e.g., Ref. [12])

$$\frac{d\sigma}{d\Omega} = |F(\mathbf{q})|^2, \quad (12)$$

with the elastic scattering amplitude,

$$|F(\mathbf{q})| = \left| F_C(\mathbf{q}) + \frac{ik}{2\pi} \int d\mathbf{b} e^{-i\mathbf{q}\cdot\mathbf{b} + 2i\eta \ln(k|\mathbf{b}|)} [1 - e^{i\chi_N(\mathbf{b})}] \right|. \quad (13)$$

Here, \mathbf{b} is the impact parameter, $\hbar k = \sqrt{(T_p/c + m_p c)^2 - (m_p c)^2}$ is the incident proton momentum, $\eta = Ze^2/\hbar v$ with the incident proton velocity $v = \hbar k c / (T_p/c + m_p c)$ is the Sommerfeld parameter,

$$F_C(\mathbf{q}) = -\frac{2\eta k}{\mathbf{q}^2} \exp \left[-2i\eta \ln \left(\frac{|\mathbf{q}|}{2k} \right) + 2i \arg \Gamma(1 + i\eta) \right] \quad (14)$$

is the amplitude of the Coulomb elastic scattering, which we approximate as a usual Rutherford scattering off a point charge, and

$$i\chi_N(\mathbf{b}) = - \int d\mathbf{r} [n_p(\mathbf{r})\Gamma_{pp}(\mathbf{b} - \mathbf{s}) + n_n(\mathbf{r})\Gamma_{pn}(\mathbf{b} - \mathbf{s})] \quad (15)$$

is the phase shift function with the projection \mathbf{s} of the coordinate \mathbf{r} on a plane perpendicular to the incident proton momentum and with the profile function Γ_{pN} of the free proton-nucleon (pN) scattering amplitude, for which we use a

simple parametrization,

$$\Gamma_{pN}(\mathbf{b}) = \frac{1 - i\alpha_{pN}}{4\pi\beta_{pN}}\sigma_{pN} \exp(-\mathbf{b}^2/2\beta_{pN}), \quad (16)$$

where σ_{pN} is the pN total cross section, $\alpha_{pN} = -\text{Im}\Gamma_{pN}(0)/\text{Re}\Gamma_{pN}(0)$, and β_{pN} is the slope parameter.

In calculating the differential cross section, we use a numerical code based on the Monte Carlo integration for evaluations of the phase shift function (15), which can be applied to an arbitrary form of nucleon distributions. The essential input in such calculations is a set of the parameters, α_{pN} , β_{pN} and σ_{pN} , that characterize the profile function (16). Here the values of α_{pN} , β_{pN} and σ_{pN} at given incident proton energy T_p are taken from Ref. [13]. We finally obtain the differential cross section as a function of the C.M. scattering angle, $\theta_{\text{c.m.}}$, from the nucleon distributions (11) in a nucleus determined as functions of the parameters L and K_0 in the macroscopic nuclear models.

We start with proton elastic scattering off stable nuclei. Figure 1 displays the elastic differential cross sections obtained for ^{58}Ni ($T_p = 1047, 400$ MeV), ^{124}Sn ($T_p = 800$ MeV), and ^{208}Pb ($T_p = 800$ MeV). In each panel the calculations were performed at $(L, K_0) = (5, 230), (50, 230), (80, 230), (50, 180), (50, 360)$ in MeV. The dependence of the obtained differential cross sections on the EOS parameters is not appreciable. Note that the present Glauber model is valid for sufficiently large T_p to justify the optical limit approximation and for sufficiently small angles to allow us to ignore the nucleon-nucleon correlations in a nucleus. By comparison with the empirical data, we may conclude that the Glauber model reasonably describes proton-nucleus elastic scattering for high incident energies ($T_p \gtrsim 500$ MeV) and for small scattering angles ($\theta_{\text{c.m.}} \lesssim 10$ deg).

Generally [17], the peak angles are related to the nuclear radius, while the peak heights are related to the diffuseness of the nuclear surface. Our nuclear model, on the other hand, predicts that the radius increases with L , while the diffuseness decreases with K_0 . It is thus important to investigate the detailed peak structure in the small scattering angle regime and its relation with L and K_0 within the present theoretical framework.

In Fig. 2, the angles and heights of the first scattering peak, calculated for 228 sets of L and K_0 ranging $0 < L < 175$ MeV and $180 \text{ MeV} \leq K_0 \leq 360$ MeV, are plotted for proton elastic scattering off stable nuclei, ^{116}Sn and ^{124}Sn , at $T_p = 800$ MeV.¹ We first note that the peak angle decreases with L . This

¹ In this paper, we define the zeroth peak as that whose angle corresponds to $\theta_{\text{c.m.}} = 0$.

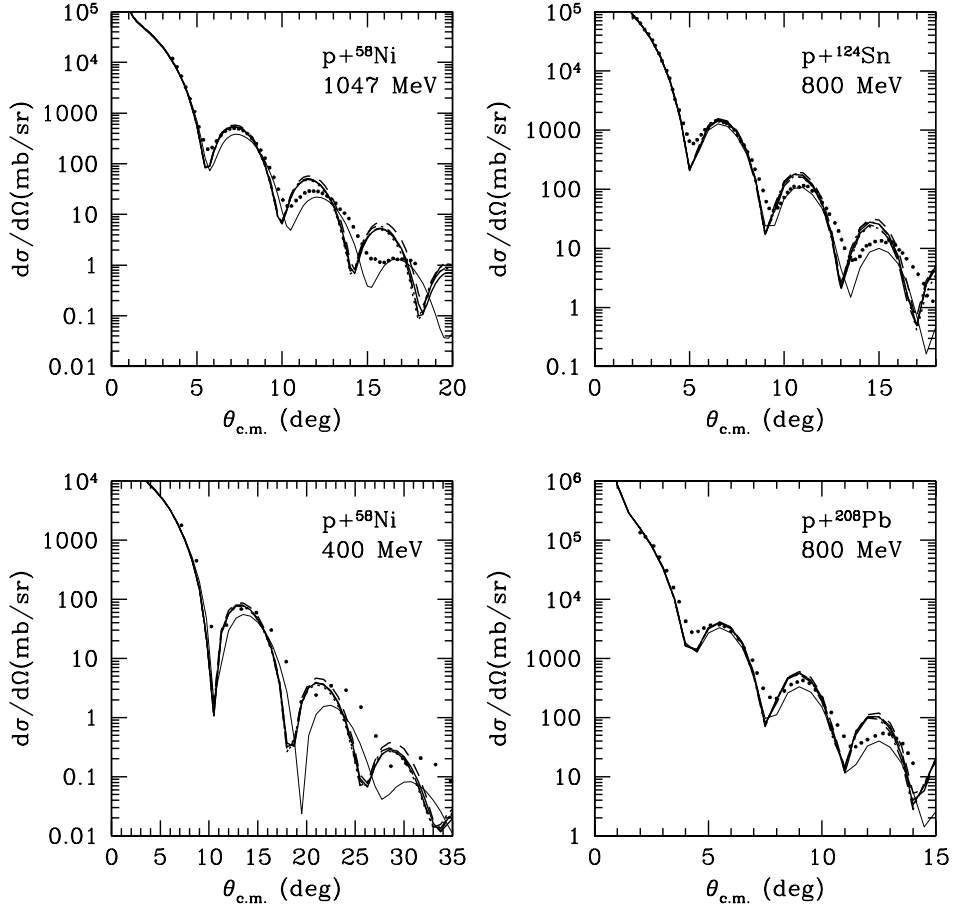


Fig. 1. Proton-nucleus elastic differential cross sections for ^{58}Ni ($T_p = 1047$, 400 MeV), ^{124}Sn ($T_p = 800$ MeV) and ^{208}Pb ($T_p = 800$ MeV). The solid, dotted, short-dashed, long-dashed and dot-dashed lines are the results calculated for $(L, K_0) = (50, 230)$, $(50, 180)$, $(50, 360)$, $(5, 230)$, $(80, 230)$ in MeV. For comparison, we also plotted the results (thin lines) calculated from the Fermi-type nucleon distributions derived in Ref. [14]. The experimental data (dots) are taken from Refs. [14,15,16].

correlation is larger for larger neutron excess, since the matter radii increase with La^2 [1]. Second, we find that the peak height increases with K_0 in a way almost independent of neutron excess. We remark in passing that there is no appreciable correlation between the peak angle and K_0 as well as between the peak height and L . This absence of appreciable correlation between the peak angle and K_0 is consistent with the fact that within the present Glauber model, the Fermi-type nucleon distributions derived by Ray et al. [14], which have larger surface diffuseness than those used in the present calculations while having similar root-mean-square neutron and proton radii, provide the angle of the first scattering peak similar to our results (see Fig. 1). We also note that K_0 (L) induced uncertainties in the peak angle (height) are typically ± 0.03

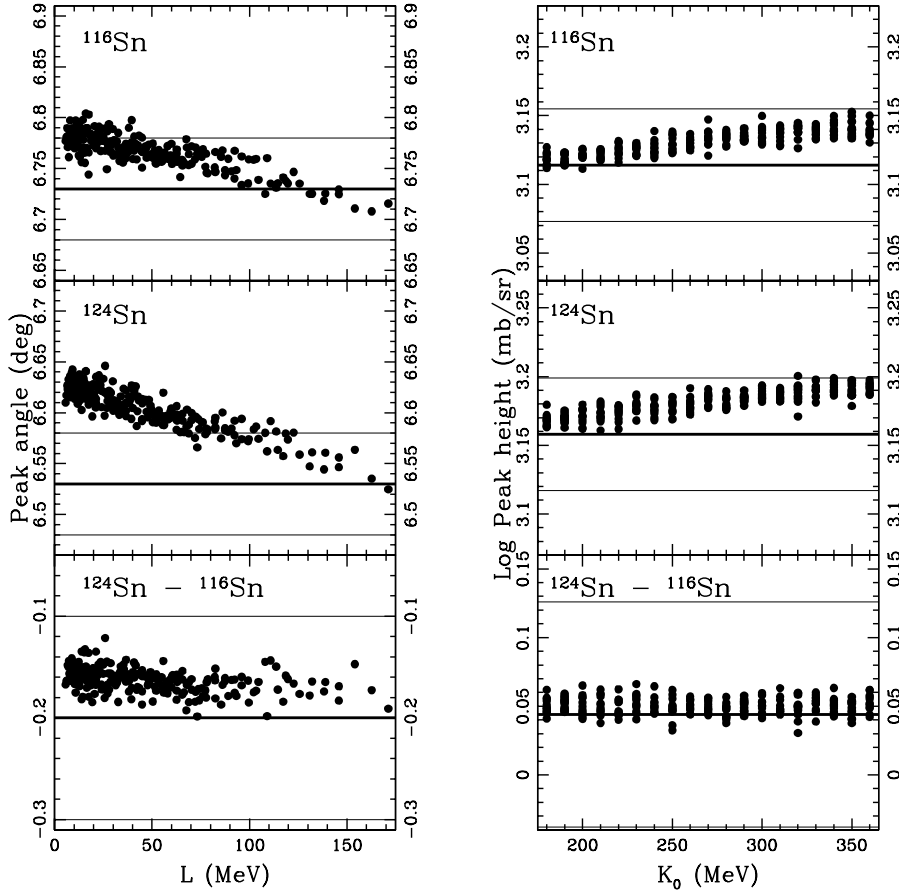


Fig. 2. The angles and heights of the scattering peak in the small angle regime, calculated as functions of L and K_0 for p - ^{116}Sn and p - ^{124}Sn elastic scattering at $T_p = 800$ MeV. The experimental angles and heights including errors (from Ref. [14]) are denoted by the horizontal lines (thick lines: central values, thin lines: upper and lower bounds).

deg (± 3 %), to which numerical errors due to the Monte Carlo integration are confined.

The empirical data for the peak angle and height, also plotted in Fig. 2, contain uncertainties in the absolute scattering angle and normalization [14], which are here taken to be ± 0.05 deg and ± 10 %, respectively. The comparison between the calculated and experimental results for the peak angles suggests a possible extraction of L . Since the calculations ignore the pairing and shell effects and the tails of the nucleon distributions, however, the comparison of the absolute values of the peak angles is accompanied by systematic errors. These errors are expected to be reduced by considering a difference in the peak angle between the ^{116}Sn and ^{124}Sn cases. The calculated values of this difference depend on L only weakly and are within the uncertainties in the

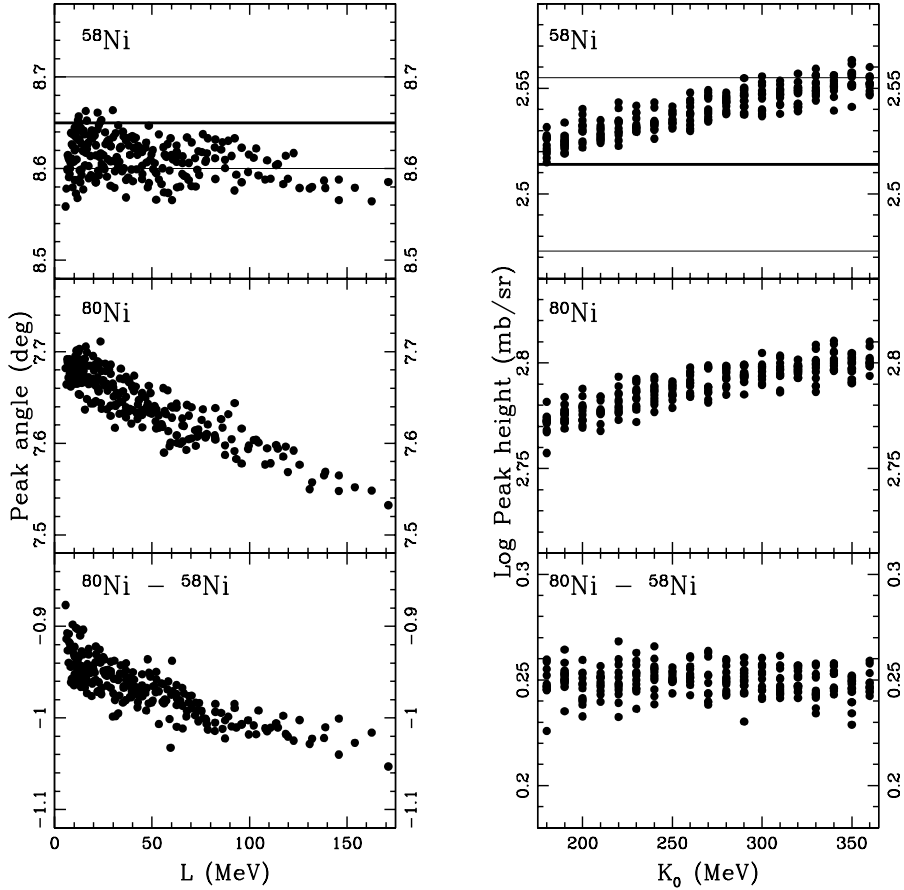


Fig. 3. Same as Fig. 2 for p - ^{58}Ni and p - ^{80}Ni elastic scattering at $T_p = 800$ MeV.

experimental value. We remark that extraction of K_0 from the peak height is difficult, since the present calculations underestimate the surface diffuseness and the values of α_{pN} , which control the peak-to-valley ratios [14], have yet to be determined uniquely.

We turn to unstable nuclei, whose beams incident on proton targets may provide elastic scattering data in future experiments. In order to examine the possibility of extracting L from the peak angles for unstable nuclei such as ^{80}Ni ($\alpha = 0.3$), we repeat the calculations for p - ^{58}Ni and p - ^{80}Ni elastic scattering at $T_p = 800$ MeV; the results for the angles and heights of the first scattering peak are exhibited in Fig. 3. We find that the L dependence of the difference in the peak angle between the ^{58}Ni and ^{80}Ni cases is appreciably large. The L induced change in the angle difference, $\Delta\theta_{\text{c.m.}}$, amounts to order 0.1 deg. This is related to the L induced change in the matter radius difference, $\Delta R_m \sim 0.1$ fm [1], by the diffraction pattern as $k\Delta\theta_{\text{c.m.}} \sim \pi\Delta R_m/R_m^2$. In order to estimate L within ± 20 MeV in the present theoretical framework, however, systematic measurements of the peak angles in the small momentum transfer regime for

various elements are desired for neutron excesses $\alpha \lesssim 0.3$ with accuracy of ± 0.01 deg.

In such an estimate of L , in which we focus on the angle of the first scattering peak, it would be useful to obtain a general relation between the peak angle and the parameters characterizing the adopted nucleon distributions within the Glauber model, as obtained by Amado et al. [17] for intermediate momentum transfers and for a Fermi distribution. It is also important to examine the predictability of the peak angle by the present scattering model. Neglect of the spin dependent part of the pN scattering amplitude and of nucleon correlations, as well as uncertainties in the values of α_{pN} , may affect the prediction of the peak angle and hence the estimate of L , although they affect the prediction of the heights of diffraction minima and maxima more remarkably [18].

We finally consider proton-nucleus total reaction cross sections, which can be calculated from the same Glauber model as used for the elastic scattering calculations. The total reaction cross section can be written as

$$\sigma_{\text{reac}} = \int d\mathbf{b} \left(1 - \left| e^{i\chi_N(\mathbf{b})} \right|^2 \right), \quad (17)$$

where χ_N is given by Eq. (15). For neutron-rich stable nuclei such as ^{208}Pb and $T_p \gtrsim 500$ MeV, we find that the total reaction cross section tends to increase with either increasing L or decreasing K_0 . This tendency stems from the fact that the reaction cross section becomes larger for larger diffuseness and radius of the nucleus. However, we have difficulty in deriving the EOS parameters from comparison with the empirical reaction cross sections even if data for unstable nuclei are accumulated. This is partly because errors in the empirical data [13] are of order or even larger than the change in the calculated reaction cross sections induced by the uncertainties in L and K_0 and partly because the surface diffuseness and the tails of the nucleon distributions, which are underestimated and ignored in the present macroscopic nuclear model, affect the prediction of the reaction cross sections.

In conclusion, by expressing the nucleon distributions in a way dependent on the EOS parameters and incorporating such distributions in the Glauber model, we calculated differential cross sections for proton-nucleus elastic scattering. At large neutron excess, we found out a large correlation between the peak angle in the small momentum transfer regime and the density symmetry coefficient L . This suggests a possible method to determine L from future systematic measurements of proton elastic scattering off unstable nuclei.

Acknowledgements

We are grateful to Dr. I. Tanihata, Dr. A. Kohama and Dr. H. Koura for helpful discussions. This work was supported in part by RIKEN Special Post-doctoral Researchers Grant No. 011-52040.

References

- [1] K. Oyamatsu, K. Iida, *Prog. Theor. Phys.* 109 (2003) 631.
- [2] H. Heiselberg, V.R. Pandharipande, *Ann. Rev. Nucl. Part. Sci.* 50 (2000) 481.
- [3] J.M. Lattimer, *Ann. Rev. Nucl. Part. Sci.* 31 (1981) 337.
- [4] P. Danielewicz, R. Lacey, W.G. Lynch, *Sci.* 298 (2002) 1592.
- [5] D.H. Youngblood, H.L. Clark, Y.-W. Lui, *Phys. Rev. Lett.* 82 (1999) 691.
- [6] J.B. Natowitz, K. Hagel, Y. Ma, M. Murray, L.Qin, R. Wada, J. Wang, *Phys. Rev. Lett.* 89 (2002) 212701.
- [7] M. Prakash, T.L. Ainsworth, J.M. Lattimer, *Phys. Rev. Lett.* 61 (1988) 2518.
- [8] C.J. Batty, E. Friedman, H.J. Gils, H. Rebel, *Adv. Nucl. Phys.* 19 (1989) 1.
- [9] L. Ray, G.W. Hoffmann, W.R. Coker, *Phys. Rep.* 212 (1992) 223.
- [10] R.J. Glauber, in: *Lectures in theoretical physics*, eds. W.E. Brittin and L.C. Dunham (Interscience, New York, 1959), Vol. 1, p. 315.
- [11] K. Oyamatsu, *Nucl. Phys. A* 561 (1993) 431.
- [12] I. Ahmad, *Nucl. Phys. A* 247 (1975) 418.
- [13] L. Ray, *Phys. Rev. C* 20 (1979) 1857.
- [14] L. Ray, W. Rory Coker, G.W. Hoffmann, *Phys. Rev. C* 18 (1978) 2641.
- [15] R.M. Lombard, G.D. Alkhozov, O.A. Domchenkov, *Nucl. Phys. A* 360 (1981) 233.
- [16] H. Sakaguchi, H. Takeda, S. Toyama, M. Itoh, A. Yamagoshi, A. Tamii, M. Yosoi, H. Akimune, I. Daito, T. Inomata, T. Noro, Y. Hosono, *Phys. Rev. C* 57 (1998) 1749.
- [17] R.D. Amado, J.-P. Dedonder, F. Lenz, *Phys. Rev. C* 21 (1980) 647.
- [18] G.D. Alkhozov, S.L. Belostotsky, A.A. Vorobyov, *Phys. Rep.* 42 (1978) 89.